Analytica Chimica Acta 1199 (2022) 339588

Contents lists available at ScienceDirect

Analytica Chimica Acta

journal homepage: www.elsevier.com/locate/aca

Paper based microfluidic platform for single-step detection of mesenchymal stromal cells secreted VEGF

Enrique Azuaje-Hualde [a], Marian M. de Pancorbo [b], Fernando Benito-Lopez [c, d, e, **], Lourdes Basabe-Desmonts [a, d, e, f, *]

[a] Microfluidics Cluster UPV/EHU, BIOMICs Microfluidics Group, Lascaray Research Center, University of the Basque Country UPV/EHU, Vitoria-Gasteiz, Spain
[b] BIOMICs Research Group, Lascaray Research Center, University of the Basque Country UPV/EHU, Vitoria-Gasteiz, Spain
[c] Microfluidics Cluster UPV/EHU, Analytical Microsystems & Materials for Lab-on-a-Chip (AMMa-LOAC) Group, Analytical Chemistry Department, University of the Basque Country UPV/EHU, Spain
[d] Bioaraba Health Research Institute, Microfluidics Cluster UPV/EHU, Vitoria-Gasteiz, Spain
[e] BCMaterials, Basque Center for Materials, Applications and Nanostructures,UPV/EHU Science Park, Leioa, Spain
[f] Basque Foundation of Science, IKERBASQUE, María Díaz Haroko Kalea, 3, 48013, Bilbao, Spain

HIGHLIGHTS

- A Structure Switching Signaling Aptamer (SSSA) was developed for the single-step detection of VEGF through fluorescence analysis.
- The SSSA was incorporated into a simple-to-use cellulose paper device, enabling the detection of 0.34 ng of the growth factor in 30 minutes.
- The paper microfluidic device was successfully applied for the quantification of VEGF secreted from a Mesenchymal Stromal Cell culture.

GRAPHICAL ABSTRACT

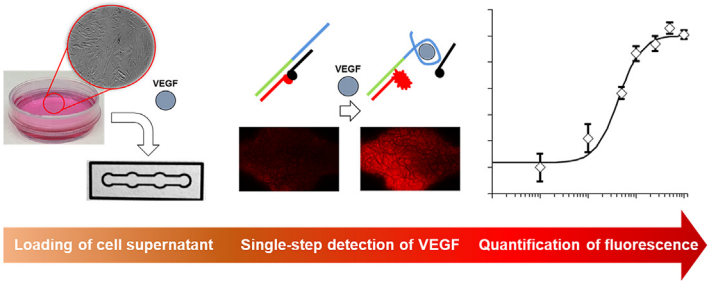

ARTICLE INFO

Article history:
Received 17 November 2021
Received in revised form
26 January 2022
Accepted 7 February 2022
Available online 9 February 2022

Keywords:
Structure switching signaling aptamer
Paper microfluidic device
Vascular endothelial growth factor
Cell secretion
Cell culture

ABSTRACT

Low cost and user-friendly paper microfluidic devices, combined with DNA-based biosensors with binding capacities for specific molecules, have been proposed for the developing of novel platforms that ease and speed-up the process of cell secretion monitoring. In this work, we present the first cellulose microfluidic paper-based analytical device for the single-step detection of cell secreted Vascular Endothelial Growth Factor through a self-reporting Structure Switching Signaling Aptamer. A three-part Structure Switching Signaling Aptamer was designed with an aptameric sequence specific for VEGF, which provides a quantifiable fluorescent signal through the displacement of a quencher upon VEGF recognition. The VEGF biosensor was integrated in cellulose paper, enabling the homogenous distribution of the sensor in the paper substrate and the detection of as low as 0.34 ng of VEGF in 30 min through fluorescence intensity analysis. As a proof-of-concept, the biosensor was incorporated in a microfluidic paper-based analytical device format containing a VEGF detection zone and a control zone, which was

* Corresponding author. Microfluidics Cluster UPV/EHU, BIOMICs Microfluidics Group, Lascaray Research Center, University of the Basque Country UPV/EHU, Vitoria-Gasteiz, Spain.
** Corresponding author. Microfluidics Cluster UPV/EHU, Analytical Microsystems & Materials for Lab-on-a-Chip (AMMa-LOAC) Group, Analytical Chemistry Department, University of the Basque Country UPV/EHU, Spain.
E-mail address: Lourdes.basabe@ehu.eus (L. Basabe-Desmonts).

https://doi.org/10.1016/j.aca.2022.339588

applied for the detection of cell secreted VEGF in the supernatant of mesenchymal stem cells culture plates, demonstrating its potential use in cell biology research.

1. Introduction

The vascular endothelial growth factor (VEGF) is a cell-secreted regulator of endothelial cells behaviour by inducing angiogenesis and vasculogenesis. Deregulations of the expression levels of VEGF are associated with several diseases, such as tumor growth, metastasis, Parkinson, Alzheimer and macular degeneration, among others, becoming both a potential therapeutic target and a disease indicator in diagnosis [1,2]. Conventional immunodetection techniques such as ELISA are often used in *in vitro* studies for the detection and quantification of secreted VEGF. However, these methods usually involve several sequential manual steps and long assay times [3]. Because of this, there is an increasing interest in the development of novel platforms able to speed-up and automatize the process of cell secretion monitoring. In the recent years, research has mainly focused on the generation of label-free or single-step techniques and systems for VEGF detection [4].

Aptamers, which are nucleic acid sequences able to specifically bind to target molecules, have been proposed as novel sensing probes for the development of a new generation of biosensors [5]. These sequences are able to adopt specific three-dimensional configurations (*i.e.* G-quadruplex structure) upon contact with the target molecules, which enables the specific capture of the analyte, presenting lower cost and higher stability than conventional antibodies [6,7]. Aptamers have been successfully designed for the detection and analysis of VEGF-isoforms [8]. Among them, the dimeric V7t1 and the 3R02 aptamers have shown high affinities for VEGF with dissociation constants (K_d) down to picomolar levels [9,10].

Several strategies have been followed in order to adapt bare aptamers into a functional biosensor for the detection of VEGF [11–13]. Among them, structure switching aptamers are a special type of three-dimensional conformation aptamers in which a double stranded sequence goes into a strand displacement upon recognition of the target molecule [14]. When the conformation change allows the production or disruption of a signal, usually a fluorescence signal, they become structure switching signaling aptamers (SSSA). The main strategy in SSSAs design usually requires short displacement strands, bound to a quencher, to partially block the recognition sequence and to absorb the excitation energy of a fluorophore bounded to the SSSA. Upon interaction with the target molecule, the release of the displacement strand allows the production of the signal, which can be correlated with the presence and quantity of the analyte [15]. Detection and analysis of several molecules have been demonstrated using SSSAs, including physiological molecules like thrombin and ATP or drugs like chloramphenicol [16,17]. In line with the SSSA design, several biosensors for VEGF are present in recent literature. For instance, Freeman et al. designed a series of optical aptasensors, specific for VEGF, based on both fluorescence and bioluminescence signals [18]. More recently, Li et al. developed a fluorescence VEGF biosensor incorporating a structure switching strand for the detection of low concentrations of the growth factor [19].

Recently, low cost and easy-to-use paper materials have been investigated for the development of new analytical devices based on RNA- and DNA-based sensors [20]. Microfluidic paper-based analytical devices (μPADs) allow to produce whole quantification assays with low volume of samples using a simple fabrication procedures, and have been extensively used in the development of protein biosensors, including commercialized HIV chips and paper ELISA tests [21,22]. In particular, cellulose and nitrocellulose substrates have been widely used for DNA purification, adsorption and analysis [23,24]. We previously reported the development of a paper microfluidic device using DNA-based sensors as DNAzymes for the colorimetric detection of ssDNA, which not only allowed to simplify the process but increased the sensitivity of the analysis when compared to the same assay in solution [25]. Aptamer-based μPADs have been developed for a wide range of detection systems, including virus, bacteria, ions and for drug analysis [26,27]. Therefore, it is ambitioned that new designed SSSA and μPADs could generate an unconventional set of technologies that get us closer to devices for multiplex detection of secreted substances from cells.

While portable microfluidics devices have been proposed for the aptamer-based detection of cell secreted VEGF [28], no analytical system has been proposed so far to unify the advantages of SSSA single-step and real time detection capabilities, the simplicity and cost-effectiveness of μPADs, and the enhanced sensitivity that can be achieved in the combination of DNA sensors and μPADs. Hence, we present here for the first time the combination of a simple-to-use μPAD for the single-step detection of secreted VEGF using a novel SSSA design (VEGF-SSSA), based on the aptamer 3R02. This approach allows to improve the detection limits of the sensing assay, thanks to the SSSA, and to simplify the analytical method, reducing cost of the assay thanks to the advantages brought by the μPAD. The VEGF-SSSA biosensor performance was investigated in terms of the sequences hybridization, specificity and sensitivity during VEGF detection both in solution and over cellulose paper substrates. Upon optimization of the process, as a proof-of-concept, the biosensor was integrated in a μPAD. Finally, the performance of the device was verified by the detection of secreted VEGF in the supernatant of mesenchymal stromal cells culture, Fig. 1.

2. Materials and methods

2.1. Materials

All oligonucleotides were synthesized by Integrated DNA Technologies (IDT, Belgium). Three oligonucleotides sequences were purchased: 5′- TGTGGGGGTGGACTGGGTGGGTACCGTCACTCGCCTCG CACCGTCC – Biotin - 3' (Aptamer DNA probe, **Apt**), 5′- GGACGGTGCGAGGCG - Cy5Sp - 3' (Fluorophore DNA probe, **F**) and 5 – IabRQ - GTGACGGTACCC - 3' (Quencher DNA probe, **Q**). The fluorophore (Cy5) had an excitation wavelength of 648 nm and an emission wavelength of 668 nm. The quencher (Iowa Black RQ) had an absorbance between 500 and 700 nm. Vascular Endothelial Growth Factor 165 (referred as VEGF onwards) was purchased from Fisher Scientific (Spain). Sodium chloride was purchased from Sigma-Aldrich (Spain). Potassium chloride and TRIS were purchased from Panreac (Spain). Streptavidin, Bovine Serum Albumin (BSA) Whatman filter paper #1 and glass covers were purchased from Sigma Aldrich (Spain). Polymethyl methacrylate (PMMA) Plexiglas 4 mm, was purchased from Evonik Industries AG (Germany). Pressure Sensitive Adhesive (PSA) ARcare 8939 was purchased from Adhesive Research (Ireland). Human adult Mesenchymal Stromal Cells were obtained from donated human hair follicles (hHF-MCSs, p6). Complete cell culture medium consisted of Dulbecco's Modified Eagle's Medium

(DMEM), Fisher Scientific (Spain), supplemented with 30% Fetal Bovine Serum (FBS), Fisher Scientific (Spain), and 10% Penicillin/Streptomycin (P/S), Fisher Scientific (Spain).

2.2. Solutions

Buffer solution consisted of sodium chloride 100 mM, potassium chloride 5 mM and TRIS 2 mM in distilled water, regulated to pH 7. All DNA probes were dissolved and then diluted in buffer solution. Three different VEGF-SSSA solutions were prepared. VEGF-SSSA solution 1 (FAptQ 1) consisted of F (1 μM), Apt (2 μM) and Q (3 μM), following a ratio 1:2:3. VEGF-SSSA solution 2 (FAptQ 2) consisted of F (200 nM), Apt (600 nM) and Q (600 nM) following a ratio 1:3:3. VEGF-SSSA solution 3 (FAptQ 3) consisted of F (200 nM), Apt (600 nM) and Q (1 μM), following a ratio 1:3:5. Two different fluorescence control solutions were prepared. Fluorescence control solution 1 (FApt 1) consisted of F (1 μM) and Apt (2 μM) and fluorescence control solution 2 (FApt 2) consisted of F (200 nM) and Apt (600 nM). Additionally, three F:Q solutions were prepared. F:Q solution 1 (FQ 1) consisted of F (1 μM) and Q (3 μM), F:Q solution 2 (FQ 2) consisted of F (200 nM) and Q (600 nM) and F:Q solution 3 (FQ 3) consisted of F (200 nM) and Q (1 μM). Finally, two solutions of F were prepared: F 1 (1 μM) and F 2 (200 nM). VEGF was dissolved and diluted in PBS in all cases. VEGF solutions 1, 2, 3, 4, 5, 6 and 7 had a concentration of 0.01, 0.1, 0.5, 1, 2.5, 5 and 10 μg mL^{-1}, respectively.

2.3. Fluorescence measurements

For solution assays: fluorescence measurements were done on a Promega Globax Multi Detection fluorometer (USA) at an excitation wavelength of 620 nm. Data were normalized to the fluorescence control intensity (F), taking the fluorescence control as the maximum possible fluorescence (100%) and calculating the percentage for each sample and the negative controls, see equation (1).

$$Normalized\ Fluorescence\ Intensity = \frac{Fluorescence\ Intensity\ Sample}{Maximum\ Fluorescence\ Intensity\ Control}\ x\ 100 \quad (1)$$

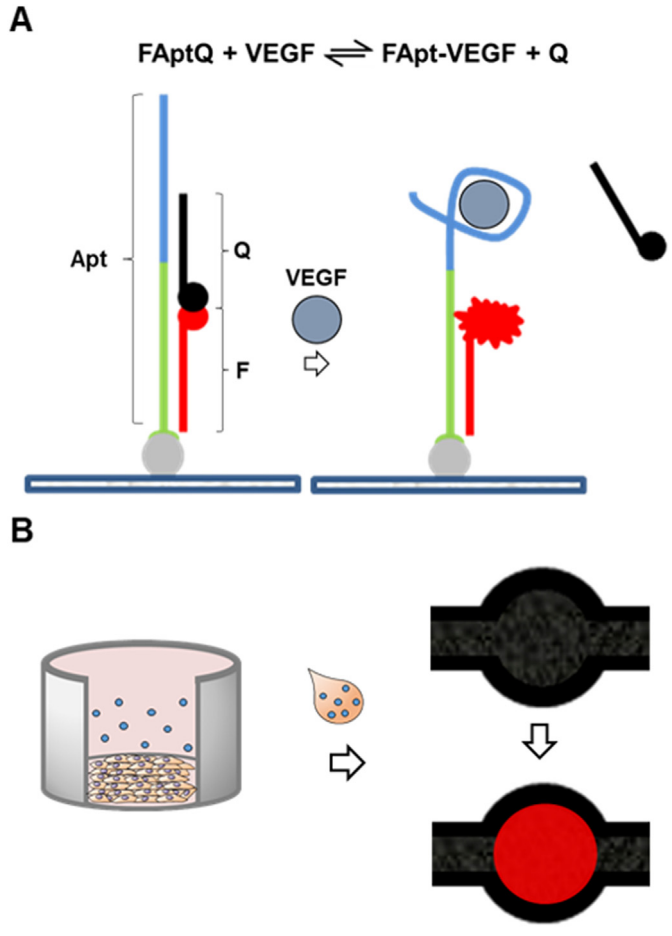

Fig. 1. Schematic representation of the VEGF detection by immobilized VEGF-SSSA. A) The binding between the aptamer probe (Apt) the fluorescence probe (F) and the quencher probe (Q) produces the quenching of the fluorophore. In the presence of VEGF, the aptamer binds to it and displaces the quencher probe, allowing the excitation and emission of the fluorophore. B) Cell supernatant can be directly loaded on a μPAD with VEGF-SSSA. Through fluorescence microscopy imaging, the concentration of VEGF can be analyzed by the quantification of the fluorescence intensity recovery produced by the interaction of VEGF with the VEGF-SSSA.

For paper assays: fluorescence microscopy images were acquired with a modified Nikon Eclipse TE2000-S inverted microscope (USA), with and adapted Andor Zyla sCMOS black and white camera (Oxford Instruments, UK). Lumencor laser 640 nm was used as light source for excitation and Quad EM filter: 446/523/600/677 with 4 TM bands: 446/34 + 523/42 + 600/36 + 677/28 4.

Four different areas of each wax-circle/detection zone (top, bottom, left-side and right-side) were imaged with a 10x objective. Each individual photograph covered an area of 0.8 mm^2. The fluorescence intensity was obtained from the NIS elements analysis software. Then, the mean value of the four images was calculated for each sample. Data were normalized to the fluorescence control (F or FApt) intensity.

3. Results and discussion

The VEGF-SSSA developed in this work (see Fig. 1 A), which is similar to the one described by R. Nutiu et al. [15], is composed of the following three sequences: A lead probe containing an elongation sequence, followed by the VEGF aptamer sequence bound to a biotin protein at its 3′ end (aptamer probe, Apt). A probe containing the complementary sequence to the first 15 nucleotides of the elongation sequence bound to a Cy5 fluorophore at its 3′ end (fluorescence probe, F). A probe containing the complementary sequence to the last 5 nucleotides of the elongation sequence and the first 7 nucleotides of the VEGF aptamer sequence bound to a Iowa Black RQ quencher at its 5' end (quencher probe, Q). On its native form, the VEGF-SSSA is formed by the bonding of F and Q to Apt (FAptQ). In presence of VEGF, Q is displaced and Apt joins VEGF to form FApt - VEGF.

A biotinylated three parts design was chosen as the best option for immobilization on substrates. While DNA has been easily immobilized in some substrates (*i.e.* cellulose or nitrocellulose), the addition of a biotin residue at the 3' end of the aptamer enables the immobilization on a streptavidin functionalized substrates. As the biotin is bound to a lead probe where the other two probes bind to, and not to the Q itself, the immobilization should not affect the performance of the SSSA as the Q can detach from the FAptQ

structure, releasing the fluorophore. The Q was designed to be complementary to both part of the elongation sequence and part of the Apt sequence. This configuration permits to anchor the Q to the Apt, to maintain the capture capabilities of the Apt and to disable any possible VEGF recognition without Q displacement.

The design of the VEGF-SSSA aimed to accomplish both the capability to detect, in a single step, low concentrations of VEGF with great specificity and the immobilization of the sensor on substrates for further implementation on microfluidics. The aptamer probe was an adaptation of the VEGF aptamer 3R02. The 3R02 was reported by Nonaka et al. [9] as mutation of the VEap121 aptamer made by *in silico* maturation, with improved sensitivity. Authors reported that the 3R02 has a good specificity for the growth factor with the lowest dissociation constants (K_d) for VEGF among all the aptamers found in literature at 300 pM so far.

3.1. VEGF-SSSA performance and VEGF detection in solution

For a correct VEGF-SSSA design, the DNA probes must form a three-dimensional structure in which only the proximity obtained between the fluorescence probe and the quencher probe, when both F and Q are assembled to the aptamer strand, results in an efficient fluorescence quenching.

First, we evaluated the quenching performance of the Q in our VEGF-SSSA. Solutions of F, FApt, FQ and FAptQ, in a ratio of 1:2:3, respectively (solution FAptQ 1, see experimental section), were analyzed in solution. The detailed experimental procedure can be found in Supporting **Information 1**.

The fluorescence signal obtained from F, FQ or FApt solutions were similar, while the signal from the FAptQ solution was 80% lower. These results indicated an efficient formation of the FAptQ duplex and quenching of the fluorescence signal (Fig. 2 A). However, contrary to our expectations, the incubation of FAptQ with the target VEGF (10 μg mL^{-1}), did not cause a change in the fluorescent signal.

Looking for the explanation of this negative result, the whole assay was carried out in the homemade PMMA well array in order to reduce the sample volume from 100 μL to 7.5 μL and so, to improve microscopy observation. Bright fluorescent aggregates were observed in the solutions containing VEGF (Fig. 2 B). Those aggregates were considered to come from the agglomeration of a FApt - VEGF complex formed after the displacement of the Q, which would explain the low fluorescence signal obtained from the FAptQ after the addition of VEGF [29].

3.2. VEGF-SSSA performance and VEGF detection on printed wax-circles

To characterize the quenching performance of Q in our VEGF-SSSA assay on cellulose paper wax-circles were printed, see Fig. 3 A. The detailed experimental procedure for the paper devices fabrication can be found in Supporting **Information 2**. The detailed experimental procedure for the VEGF detection assays on cellulose paper can be found in Supporting **Information 3**.

Solutions of FApt, FQ and FAptQ in ratios of 1:3:3 (solution FAptQ 2) and 1:3:5 (solution FAptQ 3) for F, Apt and Q, respectively, were loaded onto the cellulose paper and analyzed using fluorescence microscopy. In the case of the solutions following a 1:3:3 ratio, the FAptQ solution presented 65% lower fluorescence signal than the one obtained for the FApt solution, indicating proper assembly of the VEGF-SSSA. FQ solution presented a similar

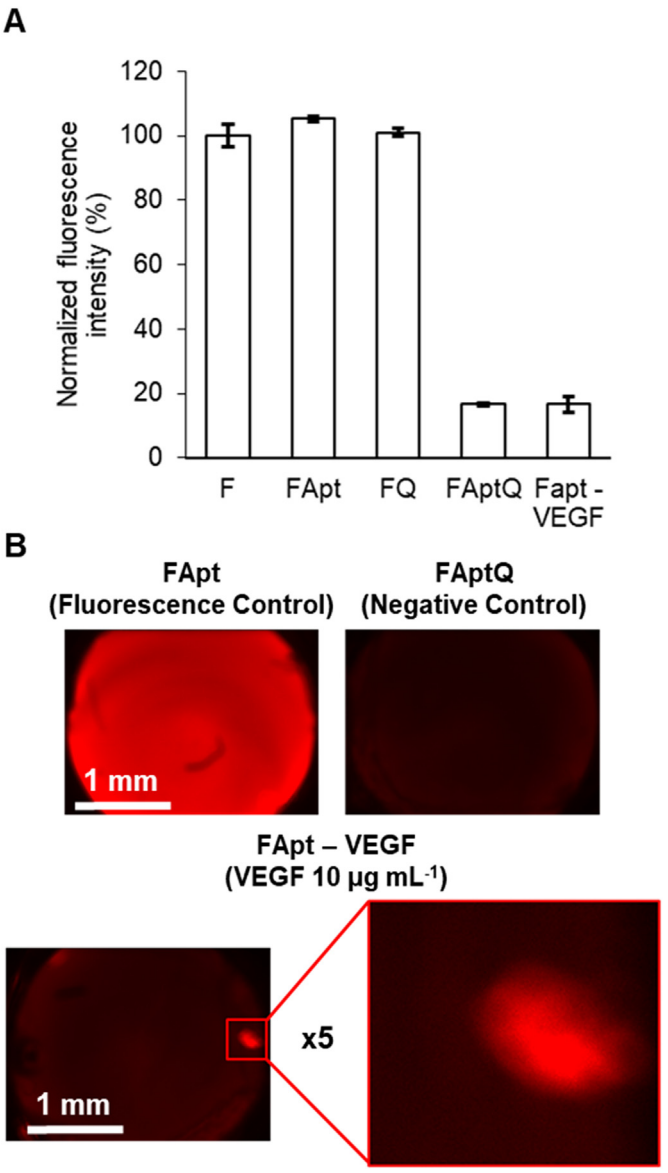

Fig. 2. Characterization of the performance of VEGF-SSSA and VEGF detection in solution. A) Plot of the fluorescence intensity for different combinations of Fluorescence probe (F), Aptamer probe (Apt) and Quencher probe (Q) solutions, as well as the formed VEGF-SSSA (FAptQ) before and after the addition of 10 μg mL^{-1} of VEGF, all normalized to F intensity. Error bars correspond to mean values ± Standard Deviation (SD, n = 3 samples per experimental condition). B) Fluorescence microscopy images of the solutions containing FApt, FAptQ and FAptQ after the addition of a 10 μg mL^{-1} VEGF solution (FApt - VEGF).

fluorescence intensity to that of FApt, indicating that without the presence of the Apt, the Q was not able to quench the fluorophore from F. In the case of the 1:3:5 ratio solutions, the sole combination of free Q with free F in the FQ solution induced a reduction of the fluorescence signal by 15%, indicating that a higher concentration of Q could quench the fluorophore even in the absence of the Apt. For that reason, the rest of the experiments were performed with the 1:3:3 ratio solutions (solution FAptQ 2), Fig. 3 B.

For the detection of VEGF in paper, either 1 μL of a 10 μg mL^{-1} VEGF solution or PBS (negative control) were incubated on the

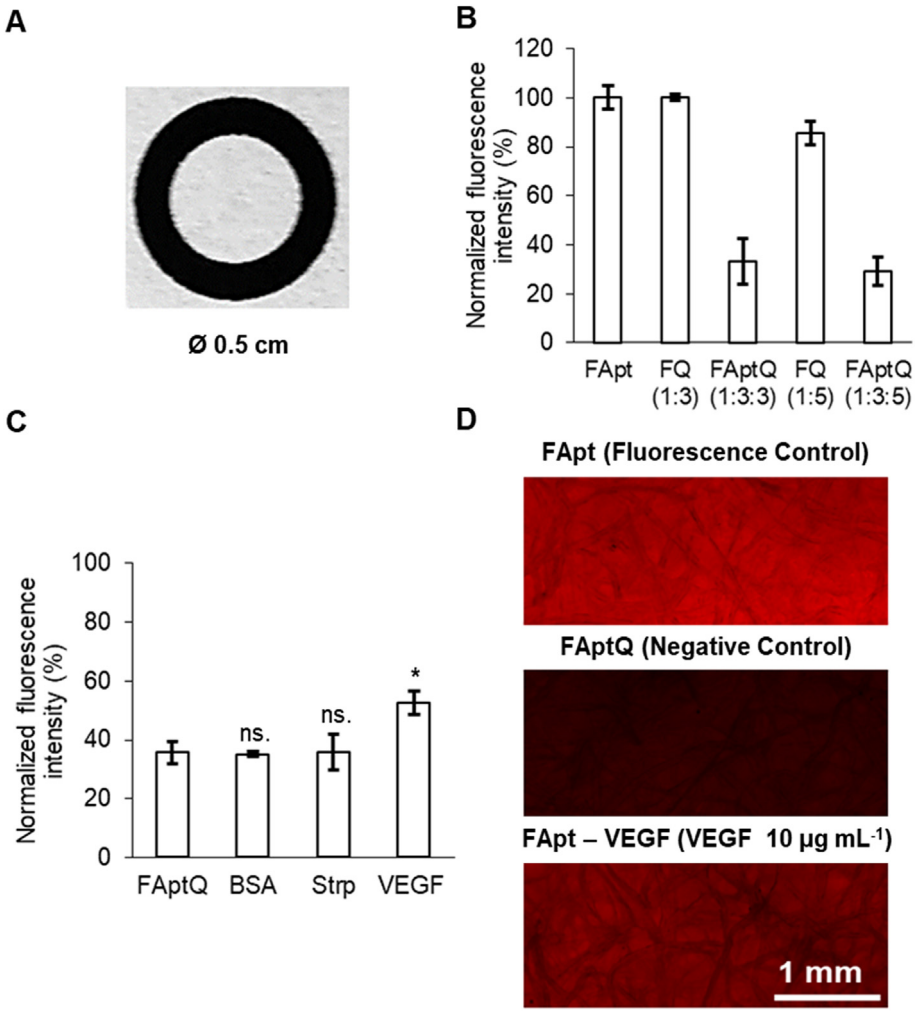

Fig. 3. VEGF-SSSA binding performance and VEGF detection on cellulose paper. A) Photographs and specifications for printed wax-circles. B) Plot of the normalized fluorescence intensity in samples containing different combinations of Fluorescence probe (F), Aptamer probe (Apt) and Quencher probe (Q) at different ratios, normalized to the fluorescence control (FApt) intensity. Error bars correspond to mean values ± SD (n = 3). C) Plot of the fluorescence intensity observed in the negative control (FAptQ) and in samples incubated with streptavidin (Strp, 100 μg mL^{-1}), BSA (100 μg mL^{-1}) and VEGF (FApt - VEGF, 10 μg mL^{-1}), normalized to the fluorescence control (FApt) intensity. Error bars mean ± SD (n = 3). Statistical significance: One-Way ANOVA, where ns. means $p > 0.05$ and ** means $p \leq 0.01$. D) Microscope images of the wax circles, showing the fluorescence obtained in the fluorescence control (FApt), the negative control (FAptQ) and the VEGF treated (FApt - VEGF) samples.

wax-circles treated with FAptQ, see experimental section, and imaged by fluorescence microscopy. The fluorescence signal increased by a 17% in the presence of the VEGF (53 ± 2%) when compared to the fluorescence signal of the negative control (36 ± 3%), indicating binding of VEGF to FApt and the formation of FApt - VEGF.

To evaluate the specificity of the assay, other proteins were tested. Either 1 μL of BSA or a streptavidin solution at high concentration (100 μg mL^{-1}) were loaded into the wax-circles with VEGF-SSSA. The concentrations of BSA and streptavidin were chosen based on the concentrations required for the blocking and binding of the SSSA to the paper microfluidic device, respectively. In both cases, the fluorescence signal remained similar to the signal of the negative controls (36 ± 2% and 36 ± 6%, respectively), Fig. 3 C.

These results confirmed the affinity of the FApt probe for VEGF, an efficient displacement of the Q producing the release of the fluorophore, and the specificity of the FApt probe for VEGF over other proteins such as BSA and streptavidin. Furthermore, the assay time in the paper substrates (30 min, see Supporting **Information 3**) was considerably lower than the assay time required in common detection techniques such as ELISA (≥ 4 h), demonstrating the capabilities of the sensor for the fast detection of the growth factor.

Contrary to the results obtained in the solution assays, fluorescence intensity in paper was more homogenous through the entire sample surface, since no agglomerates were observed. This behavior can be attributed to the spreading and deposition of the VEGF-SSSA among the cellulose surface. The higher fluorescence intensity values can also be associated with the evaporation of the reagents, as evaporation itself has been previously described to improve sensing on surfaces due to enrichment of the reagents found in the droplet, increasing the molecular interaction frequency and the reaction rates [30]. Finally, the fact that better results were obtained in the paper SSSA assay when compared to the solution assay could be explained by the fact that aptasensors often

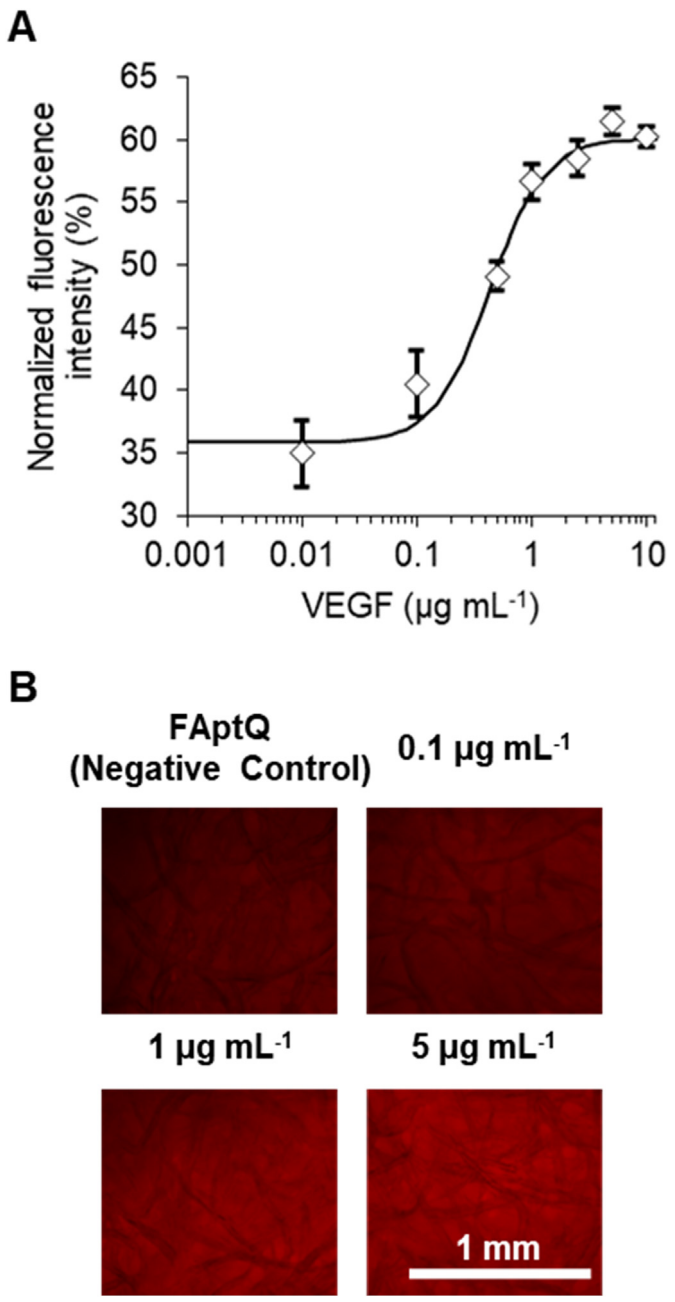

Fig. 4. Detection of different concentrations of VEGF on the VEGF-SSSA treated Whatman filter paper. A) Plot of the fluorescence intensity obtained by the incubation with different concentrations of VEGF (0.01, 0.1, 0.5, 1, 2.5, 5 and 10 µg mL^{-1}), normalized to the fluorescence control intensity. Error bars correspond to mean values ± SD (n = 4). B) Microscope images of the fluorescence obtained in paper samples treated with different concentrations of VEGF.

improve their functionality when they are immobilized on solid supports [31].

To evaluate the sensitivity of our VEGF-SSSA for VEGF, different concentrations of VEGF solution (ranging from 0.01 to 10 µg mL^{-1}) were loaded on the printed wax-circles.

As seen in Fig. 4, VEGF was detected on the paper substrate starting from the 0.1 µg mL^{-1} VEGF solution onwards. Higher fluorescence intensity, increasing from 5% to 27% from the quenched FAptQ, was observed with increasing concentrations of VEGF (40 ± 3% for the concentration of 0.1 µg mL^{-1} to 61 ± 1% for the concentration of 10 µg mL^{-1}, total normalized fluorescence intensity). A plateau was reached at the concentration of 5 µg mL^{-1}, as higher concentrations produced similar fluorescence intensities. This demonstrated the sensitivity of our VEGF-SSSA to different VEGF concentrations.

The calibration curve was fitted in a 4 Parameter Logistic non-linear regression curve, commonly used in immunoassay and aptamer-based assays [32,33]. The VEGF limit of detection (LOD, 3 x Blank values) and limit of quantification (LOQ, 3.3 x LOD) were calculated to be 137 and 455 ng mL^{-1} respectively, corresponding to 0.34 ng and 1.13 ng of VEGF respectively in our assay. The K_d calculated from the curve [34] was 336.5 ng mL^{-1} (7.5 nM).

The range of VEGF concentrations that can be detected with our VEGF-SSSA treated paper support was between 100 and 5000 ng mL^{-1}. The LOD of this technique was higher than those found in the literature, where detection of concentrations as small as picograms and fentograms per liter have been achieved [13,35,36]. Nevertheless, thanks to the reduced volume of sample required by the paper substrate (1–2.5 µL), the minimum amount of VEGF that can be detected was calculated to be as low as 350 pg. While the K_d obtained was higher than the K_d reported for the 3R02 aptameric sequence, it lied within the values obtained by other authors (between 0.3 and 20 nM) [10,37]. Furthermore, the higher concentrations found in the dynamic range of our sensor compared to that found in conventional ELISA kits, which usually covers the range of pg mL^{-1}, opens the door for the easy and direct study of more options of cell secretion studies [38–40]. Cells have a wide range of secretion profiles of VEGF, for instance in the case of MSCs, it can range from 1 to 200 ng per 10^6 cells per day depending on the stimuli [41–44]. Therefore, our technique could be useful for the monitoring of secretion during long-term MSCs cultures.

3.3. VEGF detection in µPAD

In order to integrate control and sample analysis within the same analytical platform, the VEGF-SSSA detection assay was further developed on a µPAD format. The µPAD contained four interconnected zones: a sampling zone, a VEGF detection zone, a fluorescence control zone and an endpoint, Fig. 5 A. The design of the µPAD was inspired by conventional lateral flow assays, using wax printing for the delimitation and localization of a low volume of reagents. As seen in Fig. 5 B, loading of VEGF 10 µg mL^{-1} sample produced a fluorescence recovery of 25% (60 ± 1%, total normalized fluorescence intensity) when compared with the negative controls (32.0 ± 0.9%, total normalized fluorescence intensity), which remained in their native quenched state.

The performance of the VEGF-SSSA was similar to the previous assay performed in the Whatman filter paper substrate. Furthermore, all VEGF concentrations tested produced similar intensities to those obtained in the previous assays. This demonstrated that both, flow or static modes achieved to the same results (see **Figure SI-3**). The same maximum intensity could be observed for the fluorescence controls in both samples where VEGF or buffer were loaded, indicating that the inclusion of both reservoirs did not affect the detection but simplified the methodology as the device includes a reference signal that could be analyzed alongside the sample.

This results showcase, for the first time, the possibility to incorporate SSSA biosensors within a functional µPAD. This enabled the fabrication of user-friendly and low-cost devices for the single

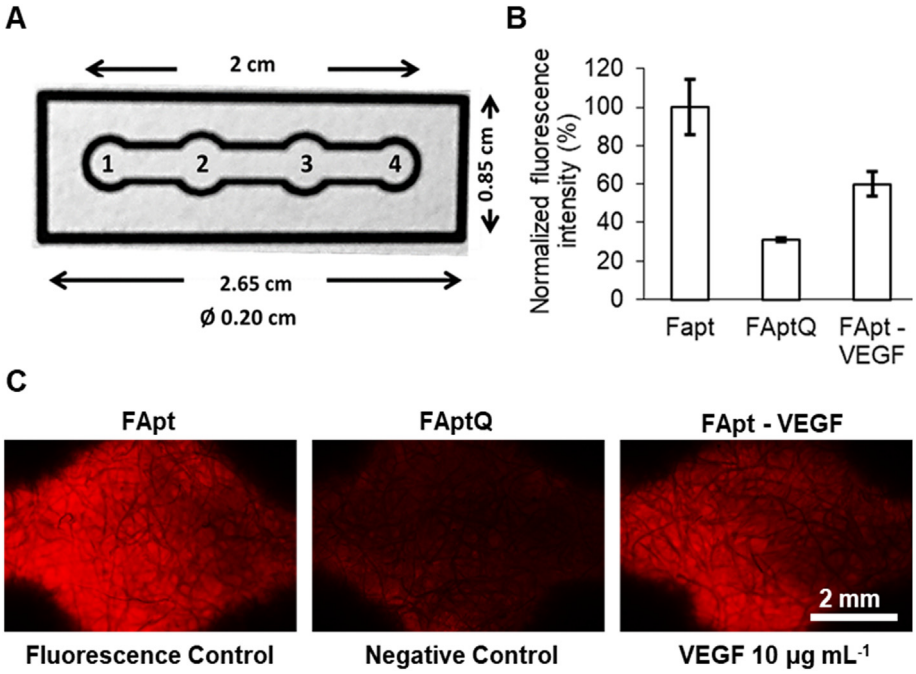

Fig. 5. Detection of VEGF in μPAD. A) Photographs and specifications for the μPAD. Numbers refer to the different zones in the μPAD: (1) sampling zone, (2) VEGF detection zone, (3) fluorescence control zone and (4) endpoint, where flow stops. B) Plot of the normalized fluorescence intensity obtained by the fluorescence control (FApt), negative control (FAptQ) and samples incubated with VEGF 10 μg mL^{-1} (FApt - VEGF), normalized to the fluorescence control (FApt) intensity. Error bars correspond to mean values ± SD (n = 3). C) Microscope images of fluorescence in the fluorescence control zone and detection zone incubated with and without VEGF.

step detection and quantification of cell secreted molecules in *in vitro* assays, presenting shorter assay times than conventional methodologies, using low volume of reagents and sample.

3.4. Cell secreted VEGF detection in μPAD

The VEGF-SSSA treated μPAD was applied for the determination of VEGF in the supernatant of hHF-MSCs culture. MSCs have interest in many biomedical applications due to their capacity of differentiation, reprogramming. MSCs have been reported to be VEGF secretors [45], which further validates their applicability.

hHF-MSCs (5 10^6 cells mL^{-1}) were cultured for 7 days on low volume of culture medium in order to promote cell secretion. After that, supernatant was loaded on the VEGF-SSSA treated μPAD and the fluorescence intensity was measured. The detailed experimental procedure can be found in Supporting **Information 4**. The normalized fluorescence intensity obtained in the μPADs, incubated with cell supernatant was 49 ± 2%, indicating that around 14% of the fluorescence was recovered from its quenched state. This would, in principle, correlate to a VEGF secretion between 60 and 100 ng per 10^6 cells per day, Fig. 6.

Our results highlighted that the VEGF secretion from cultured hHF-MSCs can be detected with the VEGF-SSSA μPAD, giving powerful insights in the capabilities of our aptasensor for its use on real cell culture scenarios. While promising, the data obtained from this analysis must be taken as indicative, as other secreted proteins by the cells such as less common VEGF subtypes might be interfering in the detection. Validation of the device with other techniques that allows precise quantification of high concentration of the growth factor is a requirement in further works.

4. Conclusions

We developed a simple to use μPAD treated with a novel VEGF-SSSA for the single-step detection and quantification of VEGF. The sensor presented good sensitivity to different concentrations of the growth factor, presenting a LOD and LOQ of 0.34 and 1.13 ng of VEGF, respectively. The immobilization of the self-reporting VEGF-SSSA on the cellulose paper improved the performance of the VEGF-SSSA and the homogeneity of the fluorescence signal. This allowed the simple and single-step quantification of the VEGF concentration by fluorescence imaging using low-cost materials and low volume of reagents and sample. The μPAD was used, as a proof of concept, for the detection of VEGF in the supernatant from hHF-MSCs cell culture.

To the best of our knowledge, this is the first time a SSSA has been integrated into a paper microfluidics device. Our approach is in concordance with previous reports, which demonstrated a powerful synergy between DNA-based biosensors and μPADs. The easiness of the fabrication method and the adaptability of wax printing to create devices of any configuration, combined with the fast and user-friendly qualities of the methodology will lead to the generation of simpler analytical tools to study biological samples.

CRediT authorship contribution statement

Enrique Azuaje-Hualde: Conceptualization, Methodology, Investigation, Writing – original draft, Writing – review & editing. **Marian M. de Pancorbo:** Writing – review & editing, Resources, Supervision, Funding acquisition. **Fernando Benito-Lopez:** Conceptualization, Methodology, Writing – review & editing, Resources, Supervision, Funding acquisition. **Lourdes Basabe-Desmonts:** Conceptualization, Writing – review & editing, Resources, Supervision, Funding acquisition.

Declaration of competing interest

The authors declare that they have no known competing financial interests or personal relationships that could have appeared to influence the work reported in this paper.

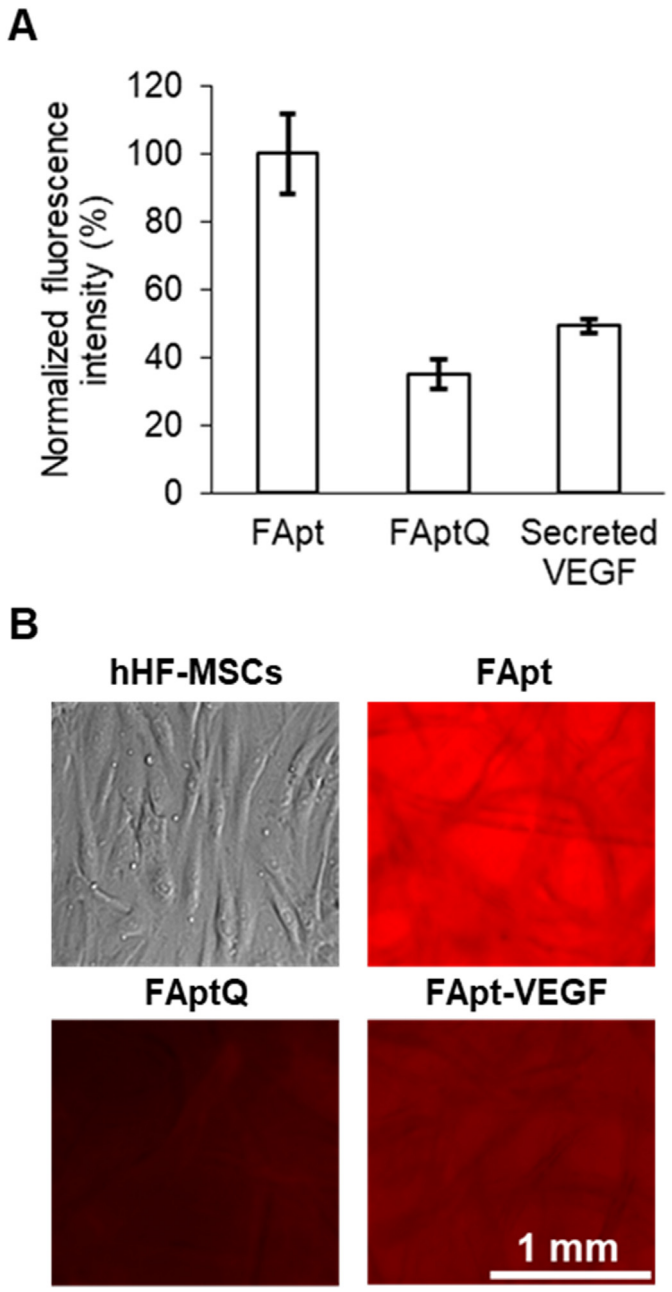

Fig. 6. Detection of secreted VEGF in hHF-MSCs supernatant. A) Plot of the normalized fluorescence intensity obtained in the fluorescence control (FApt), negative control (FAptQ) and in cell's secreted VEGF (FApt - VEGF), normalized to the fluorescence control (FApt) intensity. Error bars correspond to mean values ± SD (n = 3). B) Brightfield microscopy image of hHF-MSCs in high confluence (top left) and fluorescence microscope images of fluorescence control, negative control, and secreted VEGF incubated samples.

Acknowledgements

Authors acknowledge funding support from Basque Government, under Grupos Consolidados with Grant No. IT1271-19, from "Ministerio de Ciencia y Educación de España" under grant PID2020-120313GB-I00 /AIE /10.13039/501100011033, from the University of the Basque Country and the Spanish Government under the program "Margarita Salas" funded by "Unión Europea-Next Generation EU" . LBD and FBL personally acknowledge funds from the DNASURF (H2020-MSCA-RISE-778001) project. The authors thank for technical and human support provided by PhD Maite Alvarez from DNA Bank Service (SGIker) of the University of the Basque Country (UPV/EHU) and European funding (ERDF and ESF). Authors also wish to thank the intellectual and technical assistance from the ICTS "NANBIOSIS", more specifically by the Drug Formulation Unit (U10) of the CIBER in Bioengineering, Biomaterials & Nanomedicine (CIBER-BBN). Authors thank Dr. Alberto Gorrochategui from "Clínica Dermatológica Ercilla (Bilbao)" for providing the hair follicles from where hHF-MSCs were extracted. Finally, authors also wish to thank the technical assistance from the Nanopharmagene research group at the University of the Basque Country (UPV/EHU). FB-L and LBD acknowledge the "Red de Microfluídica Española" RED2018-102829-T.

References

[1] D.J. Hicklin, L.M. Ellis, Role of the vascular endothelial growth factor pathway in tumor growth and angiogenesis, J. Clin. Oncol. 23 (2005) 1011–1027, https://doi.org/10.1200/JCO.2005.06.081.
[2] E. Storkebaum, D. Lambrechts, P. Carmeliet, VEGF: once regarded as a specific angiogenic factor, now implicated in neuroprotection, Bioessays 26 (2004) 943–954, https://doi.org/10.1002/bies.20092.
[3] G. Sumner, C. Georgaros, A. Rafique, T. DiCioccio, J. Martin, N. Papadopoulos, T. Daly, A. Torri, Anti-VEGF drug interference with VEGF quantitation in the R& D systems human quantikine VEGF ELISA kit, Bioanalysis 11 (2019) 381–392, https://doi.org/10.4155/bio-2018-0096.
[4] M. Rothbauer, H. Zirath, P. Ertl, Recent advances in microfluidic technologies for cell-to-cell interaction studies, Lab Chip 18 (2018) 249–270, https://doi.org/10.1039/C7LC00815E.
[5] Y.S. Kim, N.H.A. Raston, M.B. Gu, Aptamer-based nanobiosensors, Biosens. Bioelectron. 76 (2016) 2–19, https://doi.org/10.1016/j.bios.2015.06.040.
[6] K. Tsukakoshi, Y. Ikuta, K. Abe, W. Yoshida, K. Iida, Y. Ma, K. Nagasawa, K. Sode, K. Ikebukuro, Structural regulation by a G-quadruplex ligand increases binding abilities of G-quadruplex-forming aptamers, Chem. Commun. 52 (2016) 12646–12649, https://doi.org/10.1039/C6CC07552E.
[7] K. Chen, J. Zhou, Z. Shao, J. Liu, J. Song, R. Wang, J. Li, W. Tan, Aptamers as versatile molecular tools for antibody production monitoring and quality control, J. Am. Chem. Soc. (2020), https://doi.org/10.1021/jacs.9b13370.
[8] H. Kaur, L.-Y.L. Yung, Probing high affinity sequences of DNA aptamer against VEGF165, PLoS One 7 (2012), e31196, https://doi.org/10.1371/journal.pone.0031196.
[9] Y. Nonaka, W. Yoshida, K. Abe, S. Ferri, H. Schulze, T.T. Bachmann, K. Ikebukuro, Affinity improvement of a VEGF aptamer by in silico maturation for a sensitive VEGF-detection system, Anal. Chem. 85 (2013) 1132–1137, https://doi.org/10.1021/ac303023d.
[10] F. Moccia, C. Riccardi, D. Musumeci, S. Leone, R. Oliva, L. Petraccone, D. Montesarchio, Insights into the G-rich VEGF-binding aptamer V7t1: when two G-quadruplexes are better than one, Nucleic Acids Res. 47 (2019) 8318–8331, https://doi.org/10.1093/nar/gkz589.
[11] W. Li, Q. Zhang, H. Zhou, J. Chen, Y. Li, C. Zhang, C. Yu, Chemiluminescence detection of a protein through the aptamer-controlled catalysis of a porphyrin probe, Anal. Chem. 87 (2015) 8336–8341, https://doi.org/10.1021/acs.analchem.5b01511.
[12] C.-L. Hsu, C.-W. Lien, C.-W. Wang, S.G. Harroun, C.-C. Huang, H.-T. Chang, Immobilization of aptamer-modified gold nanoparticles on BiOCl nanosheets: tunable peroxidase-like activity by protein recognition, Biosens. Bioelectron. 75 (2016) 181–187, https://doi.org/10.1016/j.bios.2015.08.049.
[13] O.S. Kwon, S.J. Park, J. Jang, A high-performance VEGF aptamer functionalized polypyrrole nanotube biosensor, Biomaterials 31 (2010) 4740–4747, https://doi.org/10.1016/j.biomaterials.2010.02.040.
[14] T.A. Feagin, N. Maganzini, H.T. Soh, Strategies for creating structure-switching aptamers, ACS Sens. 3 (2018) 1611–1615, https://doi.org/10.1021/acssensors.8b00516.
[15] R. Nutiu, Y. Li, Structure-switching signaling aptamers: transducing molecular recognition into fluorescence signaling, Chem. Eur J. 10 (2004) 1868–1876, https://doi.org/10.1002/chem.200305470.
[16] Z.-S. Wu, M.-M. Guo, S.-B. Zhang, Chen, J.-H. Jiang, G.-L. Shen, R.-Q. Yu, Reusable electrochemical sensing platform for highly sensitive detection of small molecules based on structure-switching signaling aptamers, Anal. Chem. 79 (2007) 2933–2939, https://doi.org/10.1021/ac0622936.
[17] X. Ma, H. Li, S. Qiao, C. Huang, Q. Liu, X. Shen, Y. Geng, W. Xu, C. Sun, A simple and rapid sensing strategy based on structure-switching signaling aptamers for the sensitive detection of chloramphenicol, Food Chem. 302 (2020) 125359, https://doi.org/10.1016/j.foodchem.2019.125359.
[18] R. Freeman, J. Girsh, A. Fang-ju Jou, J.A. Ho, T. Hug, J. Dernedde, I. Willner, Optical aptasensors for the analysis of the vascular endothelial growth factor (VEGF), Anal. Chem. 84 (2012) 6192–6198, https://doi.org/10.1021/ac3011473.
[19] J. Li, K. Sun, Z. Chen, J. Shi, D. Zhou, G. Xie, A fluorescence biosensor for VEGF detection based on DNA assembly structure switching and isothermal

amplification, Biosens. Bioelectron. 89 (2017) 964–969, https://doi.org/10.1016/j.bios.2016.09.078.
[20] G. Dutta, J. Rainbow, U. Zupancic, S. Papamatthaiou, P. Estrela, D. Moschou, Microfluidic devices for label-free DNA detection, Chemosensors 6 (2018) 43, https://doi.org/10.3390/chemosensors6040043.
[21] M.-Y. Hsu, Y.-C. Hung, D.-K. Hwang, S.-C. Lin, K.-H. Lin, C.-Y. Wang, H.-Y. Choi, Y.-P. Wang, C.-M. Cheng, Detection of aqueous VEGF concentrations before and after intravitreal injection of anti-VEGF antibody using low-volume sampling paper-based ELISA, Sci. Rep. 6 (2016) 34631, https://doi.org/10.1038/srep34631.
[22] T. Akyazi, J. Saez, J. Elizalde, F. Benito-Lopez, Fluidic flow delay by ionogel passive pumps in microfluidic paper-based analytical devices, Sensor. Actuator. B Chem. 233 (2016) 402–408, https://doi.org/10.1016/j.snb.2016.04.116.
[23] Y. Zou, M.G. Mason, Y. Wang, E. Wee, C. Turni, P.J. Blackall, M. Trau, J.R. Botella, Nucleic acid purification from plants, animals and microbes in under 30 seconds, PLoS Biol. 15 (2017), e2003916, https://doi.org/10.1371/journal.pbio.2003916.
[24] R. Shi, R.S. Lewis, D.R. Panthee, Filter paper-based spin column method for cost-efficient DNA or RNA purification, PLoS One 13 (2018), e0203011, https://doi.org/10.1371/journal.pone.0203011.
[25] E. Azuaje-Hualde, S. Arroyo-Jimenez, G. Garai-Ibabe, M.M. de Pancorbo, F. Benito-Lopez, L. Basabe-Desmonts, Naked eye Y amelogenin gene fragment detection using DNAzymes on a paper-based device, Anal. Chim. Acta 1123 (2020) 1–8, https://doi.org/10.1016/j.aca.2020.05.010.
[26] X. Weng, S. Neethirajan, Aptamer-based fluorometric determination of norovirus using a paper-based microfluidic device, Microchim. Acta 184 (2017) 4545–4552, https://doi.org/10.1007/s00604-017-2467-x.
[27] X. Cui, R. Li, X. Liu, J. Wang, X. Leng, X. Song, Q. Pei, Y. Wang, S. Liu, J. Huang, Low-background and visual detection of antibiotic based on target-activated colorimetric split peroxidase DNAzyme coupled with dual nicking enzyme signal amplification, Anal. Chim. Acta 997 (2018) 1–8, https://doi.org/10.1016/j.aca.2017.10.009.
[28] X. Lin, K.-H. Leung, L. Lin, L. Lin, S. Lin, C.-H. Leung, D.-L. Ma, J.-M. Lin, Determination of cell metabolite VEGF165 and dynamic analysis of protein–DNA interactions by combination of microfluidic technique and luminescent switch-on probe, Biosens. Bioelectron. 79 (2016) 41–47, https://doi.org/10.1016/j.bios.2015.11.089.
[29] K. Vega-Figueroa, J. Santillán, V. Ortiz-Gómez, E.O. Ortiz-Quiles, B.A. Quiñones-Colón, D.A. Castilla-Casadiego, J. Almodóvar, M.J. Bayro, J.A. Rodríguez-Martínez, E. Nicolau, Aptamer-based impedimetric assay of arsenite in water: interfacial properties and performance, ACS Omega 3 (2018) 1437–1444, https://doi.org/10.1021/acsomega.7b01710.
[30] P. Beyazkilic, A. Saateh, M. Bayindir, C. Elbuken, Evaporation-induced biomolecule detection on versatile superhydrophilic patterned surfaces: glucose and DNA assay, ACS Omega 3 (2018) 13503–13509, https://doi.org/10.1021/acsomega.8b00389.
[31] K. Urmann, J. Modrejewski, T. Scheper, J.-G. Walter, Aptamer-modified nanomaterials: principles and applications, BioNanoMaterials 18 (2017), https://doi.org/10.1515/bnm-2016-0012.
[32] D. Wu, E. Katilius, E. Olivas, M. Dumont Milutinovic, D.R. Walt, Incorporation of slow off-rate modified aptamers reagents in single molecule array assays for cytokine detection with ultrahigh sensitivity, Anal. Chem. 88 (2016) 8385–8389, https://doi.org/10.1021/acs.analchem.6b02451.
[33] C.M. Stawicki, T.E. Rinker, M. Burns, S.S. Tonapi, R.P. Galimidi, D. Anumala, J.K. Robinson, J.S. Klein, P. Mallick, Modular fluorescent nanoparticle DNA probes for detection of peptides and proteins, Sci. Rep. 11 (2021) 19921, https://doi.org/10.1038/s41598-021-99084-4.
[34] I. Jarmoskaite, I. AlSadhan, P.P. Vaidyanathan, D. Herschlag, How to measure and evaluate binding affinities, Elife 9 (2020), e57264, https://doi.org/10.7554/eLife.57264.
[35] H. Zhang, M. Li, C. Li, Z. Guo, H. Dong, P. Wu, C. Cai, G-quadruplex DNAzyme-based electrochemiluminescence biosensing strategy for VEGF165 detection: combination of aptamer–target recognition and T7 exonuclease-assisted cycling signal amplification, Biosens. Bioelectron. 74 (2015) 98–103, https://doi.org/10.1016/j.bios.2015.05.069.
[36] X.-M. Fu, Z.-J. Liu, S.-X. Cai, Y.-P. Zhao, D.-Z. Wu, C.-Y. Li, J.-H. Chen, Electrochemical aptasensor for the detection of vascular endothelial growth factor (VEGF) based on DNA-templated Ag/Pt bimetallic nanoclusters, Chin. Chem. Lett. 27 (2016) 920–926, https://doi.org/10.1016/j.cclet.2016.04.014.
[37] Y. Nonaka, K. Abe, K. Ikebukuro, Electrochemical detection of vascular endothelial growth factor with aptamer sandwich, Electrochemistry 80 (2012) 363–366, https://doi.org/10.5796/electrochemistry.80.363.
[38] A.D. Santin, P.L. Hermonat, A. Ravaggi, M.J. Cannon, S. Pecorelli, G.P. Parham, Secretion of vascular endothelial growth factor in ovarian cancer, Eur. J. Gynaecol. Oncol. 20 (1999) 177–181. http://www.ncbi.nlm.nih.gov/pubmed/10410879.
[39] C. Kut, F. Mac Gabhann, A.S. Popel, Where is VEGF in the body? A meta-analysis of VEGF distribution in cancer, Br. J. Cancer (2007), https://doi.org/10.1038/sj.bjc.6603923.
[40] F. Raimondo, M.P.M. Azzaro, G.A. Palumbo, S. Bagnato, F. Stagno, G.M. Giustolisi, E. Cacciola, G. Sortino, P. Guglielmo, R. Giustolisi, F. Di Raimondo, M.P.M. Azzaro, G.A. Palumbo, S. Bagnato, F. Stagno, G.M. Giustolisi, E. Cacciola, G. Sortino, P. Guglielmo, R. Giustolisi, Elevated vascular endothelial growth factor (VEGF) serum levels in idiopathic myelofibrosis, Leukemia 15 (2001) 976–980, https://doi.org/10.1038/sj.leu.2402124.
[41] H.-M. Cho, P.-H. Kim, H.-K. Chang, Y. Shen, K. Bonsra, B.-J. Kang, S.-Y. Yum, J.-H. Kim, S.-Y. Lee, M. Choi, H.H. Kim, G. Jang, J.-Y. Cho, Targeted genome engineering to control VEGF expression in human umbilical cord blood-derived mesenchymal stem cells: potential implications for the treatment of myocardial infarction, Stem Cells Transl. Med. 6 (2017) 1040–1051, https://doi.org/10.1002/sctm.16-0114.
[42] C.R. Ozawa, A. Banfi, N.L. Glazer, G. Thurston, M.L. Springer, P.E. Kraft, D.M. McDonald, H.M. Blau, Microenvironmental VEGF concentration, not total dose, determines a threshold between normal and aberrant angiogenesis, J. Clin. Invest. 113 (2004) 516–527, https://doi.org/10.1172/JCI18420.
[43] B.M. Beckermann, G. Kallifatidis, A. Groth, D. Frommhold, A. Apel, J. Mattern, A.V. Salnikov, G. Moldenhauer, W. Wagner, A. Diehlmann, R. Saffrich, M. Schubert, A.D. Ho, N. Giese, M.W. Büchler, H. Friess, P. Büchler, I. Herr, VEGF expression by mesenchymal stem cells contributes to angiogenesis in pancreatic carcinoma, Br. J. Cancer 99 (2008) 622–631, https://doi.org/10.1038/sj.bjc.6604508.
[44] A.I. Hoch, B.Y. Binder, D.C. Genetos, J.K. Leach, Differentiation-dependent secretion of proangiogenic factors by mesenchymal stem cells, PLoS One (2012), https://doi.org/10.1371/journal.pone.0035579.
[45] M. Makridakis, M.G. Roubelakis, A. Vlahou, Stem cells: insights into the secretome, Biochim. Biophys. Acta Protein Proteonomics 1834 (2013) 2380–2384, https://doi.org/10.1016/j.bbapap.2013.01.032.